Mineralogical Magazine, October 2008, Vol. 72(5), pp. 1011–1020

Angastonite, $CaMgAl_2(PO_4)_2(OH)_4{\cdot}7H_2O$: a new phosphate mineral from Angaston, South Australia

S. J. MILLS[1,*], L. A. GROAT[1], S. A. WILSON[1], W. D. BIRCH[2], P. S. WHITFIELD[3] AND M. RAUDSEPP[1]

[1] Department of Earth and Ocean Sciences, University of British Columbia, Vancouver, BC, Canada V6T 1Z4
[2] Geosciences, Museum Victoria, GPO Box 666, Melbourne, Victoria, 3001, Australia
[3] Institute for Chemical Process and Environmental Technology, National Research Council of Canada, Montreal Road, Ottawa, ON, Canada K1A 0R6

[*Received 16 June 2008; Accepted 11 December 2008*]

ABSTRACT

Angastonite, ideally $CaMgAl_2(PO_4)_2(OH)_4{\cdot}7H_2O$, is a newly defined mineral from the Penrice marble quarry, South Australia. The mineral occurs as snow-white crusts and coatings up to ~1 mm thick associated with minyulite, perhamite, crandallite and apatite-(CaF). The streak is white, the lustre is pearly and the estimated hardness is 2 on the Mohs scale. Angastonite forms platy crystals with the forms {010} (prominent), {101}, {10$\bar{1}$} and {100} (rare), and also occurs as replacements of an unknown pre-existing mineral. There is one cleavage direction on {010} and no twinning has been observed. Angastonite is triclinic, $P\bar{1}$, with a = 13.303(1) Å, b = 27.020(2) Å, c = 6.1070(7) Å α = 89.64(1)º, β = 83.44(1)º, γ = 80.444(8)º, V = 2150.5(4) Å^3, with Z = 6. The mineral is optically biaxial (+), with refractive indices of α = 1.566(2), β = 1.572(2) and γ = 1.584(2) and with $2V_{meas}$ = 70(2)º and $2V_{calc}$ = 71º. Orientation: X ≈ a, Y ≈ b, Z ≈ c; with crystals showing parallel extinction and no axial dispersion. D_{meas} is 2.47 g/cm^3, whilst D_{calc} is 2.332 g/cm^3. The strongest four powder-diffraction lines [d in Å, (I/I_o), hkl] are: 13.38, (100), 020; 11.05, (25), 1$\bar{1}$0; 5.73, (23), 101, 230 and 111; 8.01, (21), 130. Angastonite is likely to be related to the montgomeryite-group members and have a similar crystal structure, based on slabs of phosphate tetrahedra and Al octahedra.

KEYWORDS: angastonite, new mineral, Penrice marble quarry, Angaston, South Australia, montgomeryite, perhamite.

Introduction

THERE are several mineralogically significant phosphate deposits in the Mount Lofty Ranges of southeastern South Australia. Their hosts are low-grade phosphorite horizons within the Cambrian marine sedimentary sequence of the Kanmantoo Trough, which overlies the Proterozoic Adelaide Geosyncline (Drexel and Preiss, 1995). The deposits have been variably modified by metamorphism, followed by secondary enrichment and weathering during the Tertiary. A number of small deposits in the Angaston–Kapunda district, ~70 km northeast of Adelaide, have been mined intermittently for phosphate since the early 1900s (Jack, 1919; Johns, 1962) and have also been a source of unusual phosphate minerals for collectors and researchers (Segnit and Watts, 1981; Jones, 1983). Amongst these rare species are peisleyite (Pilkington *et al.*, 1982), aldermanite (Harrowfield *et al.*, 1981), perhamite (Mills, 2003; Mills *et al.*, 2006) and the new hydrated calcium magnesium aluminium phosphate, angastonite, the subject of this paper.

The original samples of angastonite were collected between 1988 and 1989 by Mr Vince Peisley at the Penrice marble quarry, ~2 km north of the town of Angaston (34º28′54″S, 139º2′48″E) (Fig. 1*a*,*b*). The mineral is named for the town,

* E-mail: smills@eos.ubc.ca
DOI: 10.1180/minmag.2008.072.5.1011

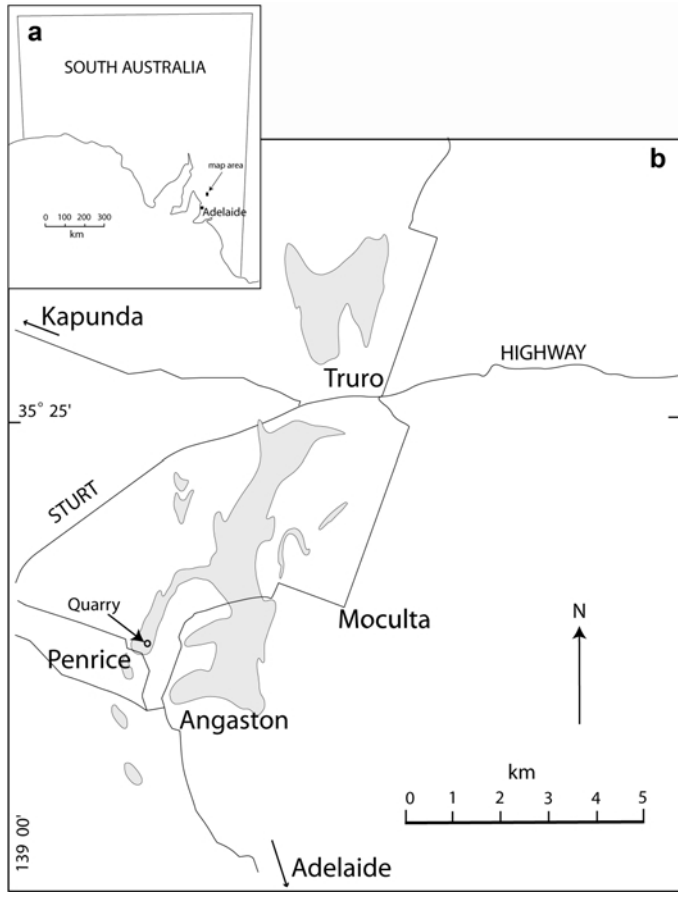

FIG. 1. (*a*) Location map of the Penrice marble quarry; and (*b*) map showing the Penrice area, with the outcrop extent of the Angaston Marble (shaded).

which was originally known as German Pass, but was later named after George Fife Angas (1789–1879), businessman and Member of Parliament of South Australia, who settled in the area in the 1850s. The mineral data and name (IMA 2008–008) have been approved by the IMA Commission on New Minerals, Nomenclature and Classification prior to publication. The type specimens are preserved in the collection of Museum Victoria, registered as M45575 and M50494.

Occurrence and geology

The larger and more prolific phosphate deposits in the district are associated with reworked phosphorite (e.g. the Moculta or Klemm's quarry; Tom's quarry at Kapunda). The more restricted phosphate mineralization at the Penrice quarry occurred in a gossanous zone above recrystallized limestone (Figs 1*b*, 2). Early descriptions by Jack (1919) of quarrying in the region extending a few kilometres north from Angaston (sections 334 and 1734, Hundred of Moorooroo) referred to extensive marble deposits, with phosphatic rock occurring in overlying dark soil and clay associated with outcrops of 'limonite' and containing residual fragments of marble. Bands of decomposed mica schist were also noted. Now named the Angaston Marble (or Kapunda Marble), the recrystallized limestone underlying the region is a lensoid reef deposit some 300 m thick, within the Early Cambrian Normanville Group. Having been metamorphosed, recrystal-

FIG. 2. Aerial photograph of the Penrice marble quarry in the late 1980s, showing the dark-brown phosphate zone (arrowed) above the marble. Photograph courtesy of Vince Peisley.

lized and folded, the marble now occurs in the near-vertical eastern limb of a south-plunging anticlinal structure. At the Penrice quarry, a 5–20 m thick contact zone of calc-silicates separates the marble from a weathered biotite-rich schist of undetermined thickness and age (A. Steinert, pers. comm.). The geological features of phosphorite found at the Penrice quarry have not been well documented, and the original phosphate mineralization in the weathering zone has been removed through the enlargement of the quarry, now the largest source of lime in South Australia. Production is ~1.1 Mt/y, most of which is used for soda ash production, with the balance for cement, construction materials, whiting and agricultural lime. Surviving specimens from the gossanous zone consist of vuggy limonitic clay enclosing small relict biotite flakes. Irregular cavities within this material are coated with compact dark-brown goethite, in turn encrusted by white phosphate mineralization. The mineralogy is quite limited, with minyulite being the most common mineral observed, in places encrusted with perhamite, crandallite or angastonite. Apatite-(CaF) (formerly fluorapatite; Burke, 2008) has also been recorded from the quarry (Mills, 2003).

Appearance and physical properties

Angastonite occurs as snow-white crusts and coatings up to ~1 mm thick on a matrix of dark-brown Fe oxyhydroxides, which have heavily impregnated soft yellowish micaceous clay (Fig. 3). Scanning electron microscope (SEM) images show several habits for angastonite, including platy crystals showing the forms {010} (prominent), {101}, {10$\bar{1}$} and {100} (rare) (Fig. 4) and aggregates of contorted tabular platelets (Fig. 5) which appear to have replaced crystals of a pre-existing phosphate mineral. Individual angastonite crystals are up to ~100 μm on edge but only ~1–2 μm thick (Fig. 4). The streak is white, the lustre is pearly and the estimated hardness is 2 (on crystal aggregates) on the Mohs scale. Individual crystal fragments are transparent, whilst intergrown aggregates appear translucent. There is one

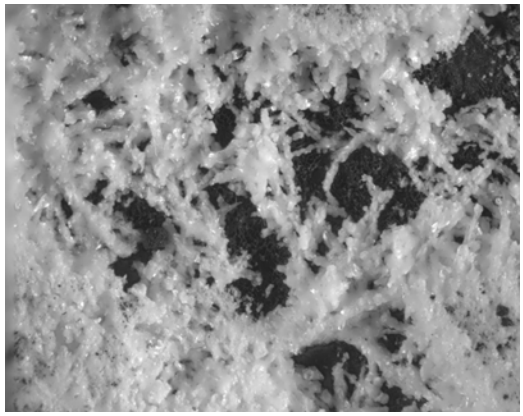

FIG. 3. Portion of the type specimen (M50494) showing intergrown crystals of angastonite on dark Fe oxy-hydroxides. The field of view is 3 mm across.

cleavage direction on {010} and no macroscopic or microscopic twinning has been observed. The measured density is 2.47 g/cm^3, determined by suspension of angastonite in methylene iodide (density 3.3 g/cm^3) diluted with acetone. The density of the methylene iodide/acetone solution was measured using a glass pycnometer and a digital balance. The density calculated on the basis of the empirical formula and unit-cell parameters (see below) is 2.332 g/cm^3.

Angastonite crystals are biaxial (+), with refractive indexes of α = 1.566(2), β = 1.572(2) and γ = 1.584(2), measured using white light, and with $2V_{meas}$ = 70(2)° and $2V_{calc}$ = 71°. Orientation: X $\approx$ *a*, Y $\approx$ *b*, Z $\approx$ *c*; with crystals showing parallel extinction. In transmitted light, angastonite is colourless, with very weak pleochroism: X = colourless, Y = colourless to pale yellow, Z = colourless; there is no axial dispersion.

Chemical composition

Seven analyses were obtained using a Cameca SX50 microprobe in WDS mode operated at 15 kV, with probe current of 2 nA and a 5 μm defocused beam, at the Department of Earth and Ocean Sciences, University of British Columbia. The results, as well as the standards used, are shown in Table 1. No other elements of atomic number Z>8 were detected. The H_2O content was determined in duplicate using a Carlo Erba 1106 automatic CHN analyser at the microanalytical unit in the Research School of Chemistry, Australian National University, and also by a Perkin Elmer Pyris 6 TGA system in the Department of Chemistry, University of British Columbia.

Angastonite is an extremely difficult mineral to analyse with an electron microprobe, due to significant instability under the electron beam. Even with a very low probe current of 2 nA and a 5 μm defocused beam, decomposition of the sample was observed. The low analytical totals for angastonite are almost certainly caused by contamination by, and instability of, the epoxy surrounding the crystals, which are only ~1–2 μm thick. Despite these major analytical problems, the major element stoichiometry remained reasonably consistent.

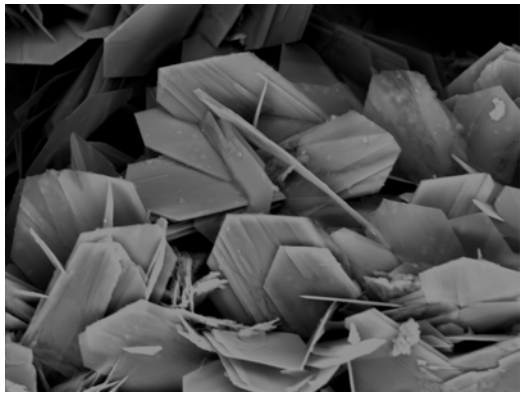

FIG. 4. SEM image of angastonite crystals on the type specimen (M50494). Crystals are up to 100 μm across on edge.

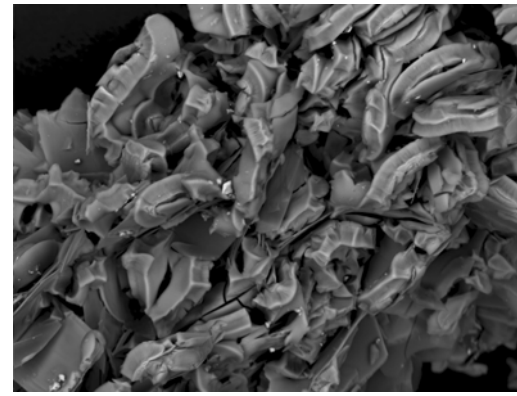

FIG. 5. SEM image showing contorted platelets of angastonite that have replaced a pre-existing phosphate (M45575). Field of view is ~100 μm across.

TABLE 1. Chemical composition of angastonite.

Constituent	Wt.%	Range	Ideal	Probe Standard
K_2O	0.09	0.04–0.16	0.09	Orthoclase ($K\alpha$, PET)
CaO	9.87	9.04–10.96	11.05	Apatite ($K\alpha$, PET)
MgO	8.17	7.61–9.14	8.02	Diopside ($K\alpha$, TAP)
Al_2O_3	18.02	16.95–20.22	20.30	Kyanite ($K\alpha$, TAP)
P_2O_5	26.11	23.06–29.27	28.25	Apatite ($K\alpha$, PET)
H_2O	31.41	30.42–32.50	32.29	–
Total	93.67		100.00	

The mean composition of angastonite corresponds to the empirical formula calculated on the basis of two phosphorus atoms is: $(Ca_{0.96}K_{0.01})_{\Sigma 0.97}Mg_{1.10}Al_{1.92}P_{2.00}O_{7.95}(OH)_{4.00}\cdot 7.47H_2O$.

The simplified formula: $CaMgAl_2(PO_4)_2(OH)_4\cdot 7H_2O$, is made up of (in wt.%): CaO 11.16, MgO 8.02, Al_2O_3 20.29, P_2O_5 28.25 and H_2O 32.28 wt.%. The formula may also be expressed as: $CaMg(H_2O)_7[Al_2(OH)_4(PO_4)_2]$ in order to emphasize the similarity to the montgomeryite formula (see discussion below).

Spectroscopy and thermogravimetric analysis

Near-infrared Raman analysis was performed using a Renishaw Imaging Microscope System 1000 (Department of Biochemistry, University of British Columbia), with an RL785 diode laser at a wavelength of 785 nm, a RenCam CCD detector and Renishaw WiRE Version 1.3.30 instrument control software. The data were analysed using *Galatic Grams/32* Version 4.14 software. Prior to data acquisition, a spectral calibration was carried out using the Raman spectrum obtained from a silicon wafer.

Angastonite shows several PO_4 vibrational modes analogous to those found in other phosphates, e.g. apatite (Sauer *et al*., 1994). The PO_4 ν_3 occurs at 1159 cm^{-1}, PO_4 ν_1 stretching mode at 988 cm^{-1}, PO_4 ν_4 bending mode at 630 cm^{-1}, PO_4 ν_4 stretching modes at 539 and 502 cm^{-1} and a PO_4 ν_2 at 415 cm^{-1}. Raman spectroscopy confirmed the absence of carbonate in the crystal structure of angastonite.

Simultaneous TGA analyses were obtained from 4.96 mg of hand-picked material from the co-type specimen M45575. The sample was analysed using a Perkin Elmer Pyris 6 TGA (Department of Chemistry, University of British Columbia) over the temperature range 30–900ºC, with a heating rate of 5ºC/min. Angastonite loses its water molecules over two steps (Fig. 6) between 30 and 170ºC (~$5.3H_2O$) and 170 and 390ºC (~$1.7H_2O$ plus hydroxide). Above 390ºC, there are several ill-defined steps where angastonite slowly dehydroxylates. Total mass loss for angastonite is 32.5%, which corresponds quite well to the amount of water both calculated from the ideal formula (32.28 wt.%) and determined by CHN analysis (31.4 wt.%).

X-ray diffraction

Single-crystal X-ray studies could not be carried out on angastonite. A number of attempts using a Bruker X8 diffractometer were made to obtain crystals suitable for structure determination. In all cases, only powder lines were observed in the diffraction patterns. Several samples were also sent to the Advanced Light Source (ALS), Berkeley, California, but it was not possible to obtain a data set.

X-ray diffraction data were initially obtained using a slurry of angastonite mixed with anhydrous ethanol and dispersed on a zero-background plate. Data were collected on a Siemens D5000 θ-2θ diffractometer equipped with a VÅNTEC-1 detector. The X-ray powder data show severe preferred orientation on the (0*k*0) reflection, leading to an I/I_o of <1 for almost all reflections and confirmed the presence of cleavage.

The sample was then mounted in a 0.3 mm quartz capillary. The data were collected on a Bruker D8 Advance Cu-$K\alpha$ diffractometer with a focusing primary mirror and a VÅNTEC PSD detector. Due to the small sample size, an 8-mm Debye slit was used to reduce scattering from the empty capillary. Both conventional and pseudo-variable count-time datasets were obtained from

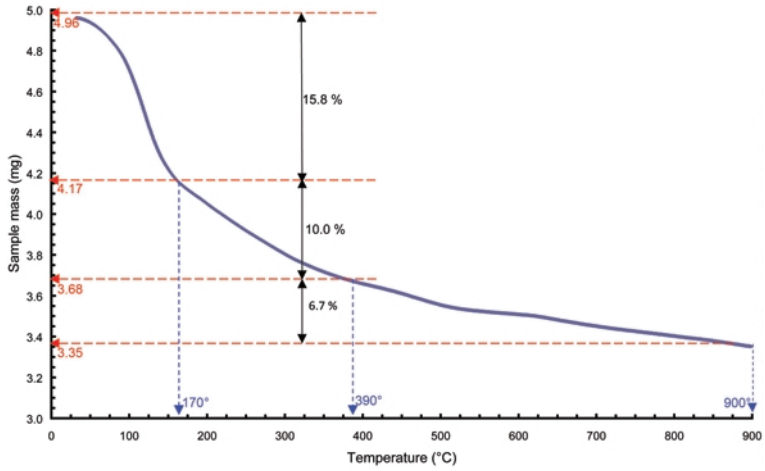

FIG. 6. Thermogravimetric results for angastonite.

the sample. The variable count (VCT) data were taken in five sections using increasing count times and step sizes with increasing two-theta angle to maximize the signal-to-noise in the information-rich, high-angle region. The counting times employed were (2θ range, step size, time per step):

5–13°,	0.0142°,	6s;
13–34°,	0.0142°,	8s;
34–56.2°,	0.0214°,	12s;
56.2–80°,	0.0284°,	16s;
80–115°,	0.0365°,	20s.

VCT data were also obtained for angastonite at 87 K using a custom-built liquid-nitrogen cryo-flow system. A 4-mm Debye slit was used to ensure that data were collected only from the constant-temperature region in the nitrogen gas stream. The data-collection regime was the same as above, except the counting time for each segment was increased by 50%.

The scattering from the capillary was subtracted from the data using a blank dataset. The datasets were rescaled and merged into single xye format datasets. The indexing was carried out using *TOPAS* version 4.1 (Bruker AXS, 2008). Single-peak fitting was used to provide input for the LSI indexing routine in *TOPAS*. Symmetries from tetragonal to triclinic were surveyed, with varying ratios of observed to calculated reflections. The top 100 cells with the best goodness-of-fit were input into an automated Pawley fitting routine to determine which cells had the best fit to the experimental data. The best-fitting cells were examined in terms of calculated densities and Z values to narrow the possibilities further.

Angastonite was determined to be triclinic, $P\bar{1}$, with the unit-cell parameters: a = 13.303(1) Å, b = 27.020(2) Å, c = 6.1070(7) Å, α = 89.64(1)°, β = 83.44(1)°, γ = 80.444(8)°, V = 2150.5(4) Å^3, with Z = 6 (Table 2; Fig. 7*a*). At 87 K, angastonite has the unit-cell parameters: a = 13.259(2) Å, b = 26.980(4) Å, c = 6.1268(9) Å, α = 89.17(1)°, β = 83.13(2)°, γ = 80.490(9)° and V = 2146.2(6) Å^3 (Fig. 7*b*). From the unit-cell parameters, a:b:c is 0.4923:1:0.2260 at room temperature and 0.4914:1:0.2271 at 87 K. The calculated density based on the room-temperature, unit-cell parameters is 2.332 g/cm^3, whilst the Gladstone–Dale compatibility index (Mandarino, 1981) is −0.013, categorized as superior.

Relationship to montgomeryite-group members

Currently, we have not been able to solve the crystal structure of angastonite; however, using simulated annealing techniques within *TOPAS*, potential partial structures show similarities to that of montgomeryite (Moore and Araki, 1974), whereby chains of Al octahedra are corner-linked to equivalent chains of PO_4 tetrahedra. In montgomeryite and vauxite, this results in a slab oriented parallel to the (010) plane. This slab is responsible for the perfect cleavage on {010} in montgomeryite and is a probable reason for the {010} cleavage found in angastonite.

For montgomeryite and vauxite, these chains and enveloping tetrahedra lead to compositions $[Al_4(OH)_4(PO_4)_6]$ and $[Al_4(OH)_4(H_2O)_4(PO_4)_4]$, respectively. In angastonite, a likely slab

TABLE 2. X-ray powder-diffraction data for angastonite. The five strongest lines are in bold.

h	k	l	I_{obs}	d_{obs}	d_{calc}
0	2	0	**100**	13.38	13.32
1	$\bar{1}$	0	**25**	11.05	11.01
1	2	0	13	10.22	10.20
1	3	0	**21**	8.01	7.98
2	$\bar{1}$	0	8	6.06	6.10
0	0	1			6.07
1	0	1			5.76
2	3	0	**23**	5.73	5.73
1	1	1			5.70
1	$\bar{4}$	0			5.57
1	$\bar{1}$	1	8	5.57	5.56
0	$\bar{2}$	1			5.55
2	$\bar{2}$	0			5.50
2	4	0	4	5.11	5.10
1	$\bar{1}$	$\bar{1}$			5.10
0	3	1	2	4.992	4.979
1	3	1			4.973
1	$\bar{2}$	$\bar{1}$	2	4.754	4.776
2	1	1			4.737
2	5	$\bar{1}$	2	3.506	3.506
1	$\bar{7}$	0			3.500
3	$\bar{2}$	1	2	3.483	3.481
3	3	$\bar{1}$	2	3.333	3.289
3	5	1	1	3.288	3.277
3	$\bar{1}$	$\bar{1}$			3.274
1	$\bar{8}$	0	2	3.109	3.105
4	0	1	2	3.007	3.018
0	$\bar{1}$	2			3.018
4	5	0			3.012
0	1	2			3.009
3	$\bar{3}$	$\bar{1}$			3.006
1	$\bar{1}$	2			3.004
2	7	$\bar{1}$			3.001
1	9	0			2.997
4	3	1			2.996
0	2	2	4	2.940	2.949
1	$\bar{2}$	2			2.940
0	$\bar{8}$	1			2.936
1	3	2	**19**	2.888	2.892
2	$\bar{6}$	$\bar{1}$			2.890
3	8	0			2.885
3	$\bar{5}$	1			2.884
1	0	$\bar{2}$			2.882
0	$\bar{3}$	2			2.882
2	9	0			2.882
2	1	2			2.881
1	1	$\bar{2}$			2.881
2	0	2			2.879
4	$\bar{2}$	1			2.854
2	2	2	2	2.856	2.851
1	$\bar{1}$	$\bar{2}$			2.851
2	$\bar{7}$	1	17	2.819	2.815
4	5	1			2.810
2	3	2	2	2.784	2.789
1	$\bar{2}$	$\bar{2}$			2.789
1	$\bar{9}$	0			2.788
1	4	2			2.787
2	$\bar{8}$	0			2.784
1	3	$\bar{2}$			2.782
2	$\bar{2}$	2			2.779
4	$\bar{3}$	1	4	2.736	2.737
4	3	$\bar{1}$			2.735
1	$\bar{4}$	2			2.733
4	4	$\bar{1}$	2	2.671	2.677
0	$\bar{9}$	1			2.674
3	8	1			2.674
1	9	$\bar{1}$			2.673
2	$\bar{7}$	$\bar{1}$			2.672
1	5	2			2.665
2	$\bar{8}$	1	2	2.588	2.590
1	5	$\bar{2}$			2.589
3	3	2			2.588
2	$\bar{4}$	2			2.586
2	3	$\bar{2}$			2.584
1	10	$\bar{1}$	2	2.457	2.457
1	11	0			2.456
5	$\bar{1}$	1			2.455
6	5	1	2	2.089	2.090
6	$\bar{2}$	0			2.089
4	$\bar{8}$	1			2.088
2	14	0	4	1.913	1.914
4	$\bar{7}$	2			1.913
4	$\bar{10}$	0			1.913
2	11	2			1.912
6	$\bar{2}$	$\bar{1}$			1.910
2	11	$\bar{2}$	4	1.857	1.858
7	5	0			1.856
4	$\bar{1}$	3	4	1.797	1.800
2	5	$\bar{3}$			1.800
3	14	1			1.797
2	7	3			1.797
2	$\bar{6}$	3			1.796
6	$\bar{7}$	0	2	1.765	1.764
7	$\bar{3}$	0			1.764
6	$\bar{5}$	$\bar{1}$			1.764
4	$\bar{7}$	$\bar{2}$	4	1.755	1.756
7	8	0			1.754
3	6	$\bar{3}$	2	1.679	1.680
0	$\bar{9}$	3			1.680

composition is $[Al_2(OH)_4(PO_4)_2]$, based on this topology. If angastonite has a topology similar to that of montgomeryite, then the chemical formula for angastonite can be revised to reflect this morphology. In montgomeryite and vauxite, the slab composition is separated from the metal octahedra, Ca polyhedra and water molecules. On this basis, angastonite could have the following formula: $CaMg(H_2O)_7[Al_2(OH)_4(PO_4)_2]$.

Angastonite has many similar features to montgomeryite (Table 3), the most striking being the ~6 Å *c* axis, cleavage on {010} and similar chemical elements. However, the properties, in particular the X-ray diffraction, are distinct enough to define unambiguously angastonite as a separate species.

Paragenesis

Angastonite formed under supergene (weathering) conditions at an uncertain time. Deep weathering in rocks of the Mount Lofty Ranges and

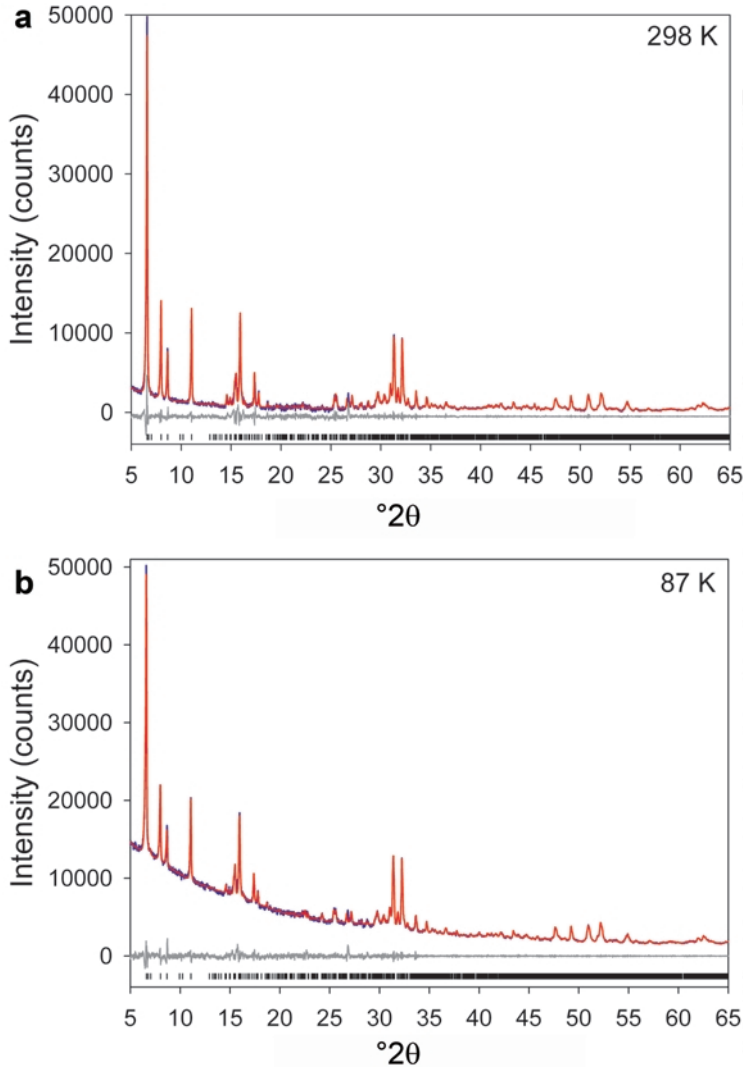

FIG. 7. Fit (red line) to the experimental capillary powder pattern (blue line) for angastonite at room temperature (*a*) and 87 K (*b*) between 5 and 65º 2θ. The difference curve is in grey and the tick marks show the Bragg reflection positions.

TABLE 3. Comparison data for angastonite, montgomeryite and vauxite. Data compiled from Anthony *et al*. (2000).

Formula	Angastonite $CaMg(H_2O)_7[Al_2(OH)_4(PO_4)_2]$	Montgomeryite $Ca_4Mg(H_2O)_{12}[Al_4(OH)_4(PO_4)_6]$	Vauxite $Fe_2(H_2O)_4[Al_4(OH)_4(H_2O)_4(PO_4)_4](H_2O)_4$
Crystallography			
Space group	$P\bar{1}$	$C2$	$P\bar{1}$
a (Å)	13.303(1)	10.004–10.023	9.142(3)
b (Å)	27.020(2)	24.083–24.121	11.599(3)
c (Å)	6.1070(7)	6.235–6.243	6.158(2)
α (°)	89.64(1)	–	98.29(2)
β (°)	83.44(1)	91.55–91.60	91.93(3)
γ (°)	80.444(8)	–	108.27(3)
V (Å^3)	2150.5(4)	~1500	611.42
Z	6	2	2
5 strongest lines in the powder pattern	13.38 (100), 11.05 (25), 5.73 (23), 8.01 (21), 2.888 (19)	12.0 (100), 5.11 (65), 2.895 (45), 2.580 (30), 2.874 (25)	10.85 (100), 5.457 (20), 5.908 (12), 2.881 (12), 2.596 (12)
D_{meas}, D_{calc}	2.47, 2.332	2.53(5), 2.523	2.39–2.40, 2.40
Cleavage	{010}	{010}	none noted
Optics			
α	1.566(2)	1.572(2)	1.551(3)
β	1.572(2)	1.578(2)	1.555(3)
γ	1.584(2)	1.582(2)	1.562(3)
Opt. character	positive	negative	positive
2V(°) (meas.), (calc.)	70(2), 71	75(10), 78	32, 74
Orientation	$X \approx a$, $Y \approx b$, $Z \approx c$	$Z = b$	Z ~ perp. {010}
X (colour)	colourless	colourless to pale green and light orange brown	colourless
Y (colour)	colourless to pale yellow	colourless to pale magenta-pink	blue
Z (colour)	colourless	colourless to light orange-brown	colourless
Absorption	r = v	r < v	r > v, marked

elsewhere may be due to continuous weathering and reworking over long time periods (Benbow *et al*., 1995). However, the angastonite-bearing suite is likely to represent the youngest phase of phosphate deposition, and may be associated with the extensive development of karst features on limestones during the late Tertiary and throughout the Quaternary (Sheard and Smith, 1995). Under these conditions, the underlying marble provided Ca and P for the phosphate assemblage. The presence of a number of Ca-Al phosphates within the same environment, commonly in overgrowth configurations, indicates that these elements were in elevated concentrations in groundwater, and suggests that small fluctuations in other elements such as Mg, Na and K governed which mineral precipitated. It is also possible that angastonite has resulted from the 'desilicification' of perhamite, or the alteration of montgomeryite, which has not been recorded from the quarry so far.

Acknowledgements

The Principal Editor, Mark Welch, and Frédéric Hatert and Gunnar Raade, provided helpful comments on the manuscript. Aaron Steinert (Project Manager, Penrice Quarry) provided information on the geology of the locality, as well as photographs of the quarry. Vince Peisley provided additional reference samples and photographs of the phosphate deposits. Xavier Roy and Mark MacLachlan (Department of Chemistry, UBC) are thanked for the thermogravimetric analysis and Marcia Yu (Department of Biochemistry, UBC) is thanked for providing access to the Raman microscope. This work was supported, in part, by NSERC Discovery Grants to LAG and MR, and Research Tools and Instruments Grants to MR.

References

Anthony, J.W., Bideaux, R.A., Bladh, K.W. and Nichols, M.C. (2000) *Handbook of Mineralogy,*

Volume IV. Arsenates, Phosphates, Vanadates. Mineral Data Publishing, Tucson, AZ, USA. 680 pp.

Benbow, M.C., Callen, R.A., Bourman, R.P. and Alley, N.F. (1995) Deep weathering, ferricrete and silcrete. Pp. 201–207 in: *The Geology of South Australia*, *vol. 2*, *The Phanerozoic* (J.F. Drexel, and W.V. Preiss, editors), Bulletin **54**, Geological Survey of South Australia.

Bruker AXS (2008) *TOPAS*, V4.1, Bruker AXS, Karlsruhe, Germany.

Burke, E.A.J. (2008) Tidying up mineral names: an IMACNMNC scheme for suffixes, hyphens and diacritical marks. *Mineralogical Record*, **39**, 131–135.

Drexel, J.F. and Preiss, W.V. (editors) (1995) *The Geology of South Australia, vol. 2, The Phanerozoic*, Bulletin **54**, Geological Survey of South Australia.

Harrowfield, J.R., Segnit, E.R. and Watts, J.A. (1981) Aldermanite, a new magnesium aluminium phosphate. *Mineralogical Magazine*, **44**, 59–62.

Jack, R.L. (1919) *The phosphate deposits of South Australia*. Bulletin **7**, Geological Survey of South Australia.

Johns, R.K. (1962) South Australian rock phosphate deposits. *Mining Review Adelaide*, **114**, 22–30.

Jones, J.B. (1983) Phosphate deposits of the Mount Lofty and Middleback Ranges. In: *Phosphate occurrences in Australia*, *Abstract volume*. The Mineralogical Societies of New South Wales, South Australia and Victoria, Annual Seminar, Adelaide, Australia.

Mandarino, J.A. (1981) The Gladstone-Dale relationship: Part IV. The compatibility concept and its application. *The Canadian Mineralogist*, **19**, 441–450.

Mills, S.J. (2003) A note on perhamite from the Moculta (Klemms) phosphate quarry, South Australia. *Australian Journal of Mineralogy*, **9**, 43–45.

Mills, S.J., Grey, I.E., Mumme, W.G. and Bordet, P. (2006) The crystal structure of perhamite. *Mineralogical Magazine*, **70**, 201–209.

Moore, P.B. and Araki, T. (1974) Montgomeryite, $Ca_4Mg(H_2O)_{12}[Al_4(OH)_4(PO_4)_6]$: its crystal structure and relation to vauxite, $Fe_2^{2+}(H_2O)_4[Al_4(OH)_4(H_2O)_4(PO_4)_4]\cdot 4H_2O$. *American Mineralogist*, **59**, 843–850.

Pilkington, E.S., Segnit, E.R. and Watts, J.A. (1982) Peisleyite, a new sodium aluminium sulphate phosphate. *Mineralogical Magazine*, **46**, 449–452.

Sauer, G.R., Zunic, W.B., Durig, J.R. and Wuthier, R.E. (1994) Fourier transform Raman spectroscopy of synthetic and biological calcium phosphates. *Calcified Tissue International*, **54**, 414–420.

Segnit, E.R. and Watts, J.A. (1981) Mineralogy of the rock phosphate deposit at Moculta, South Australia. *Australian Mineralogist*, **35**, 179–186.

Sheard, M.J. and Smith, P.C. (1995) Karst and mound spring deposits. Pp. 257–261 in: *The Geology of South Australia*, v*ol. 2, The Phanerozoic*, (J.F. Drexel and W.V. Preiss, editors), Bulletin **54**, Geological Survey of South Australia.